

DETERMINATIVE ROLE OF EXCHANGE CATION AND CHARGE DENSITY OF
SMECTITES ON THEIR ADSORPTION CAPACITY AND AFFINITY FOR
AFLATOXIN B₁

A Thesis

by

LIAN LIU

Submitted to the Office of Graduate Studies of
Texas A&M University
in partial fulfillment of the requirements for the degree of

MASTER OF SCIENCE

Chair of Committee,	Youjun Deng
Committee Members,	Scott A. Senseman
	Sergio C. Capareda
Head of Department,	David Baltensperger

August 2013

Major Subject: Soil Science

Copyright 2013 Lian Liu

ABSTRACT

Bentonite clays have long been used as additives in animal feed, aiming to improve pellet quality and prevent caking. Certain bentonites are also capable of deactivating aflatoxin B₁ (AfB₁) in feed by adsorption, therefore, detoxifying the feed. However, a 10-fold difference in adsorption capacity has been observed among selected bentonites. The major mineralogical and chemical properties of smectites in determining their adsorption capacities for AfB₁ are still poorly understood. Improved knowledge of the key controlling factors of aflatoxin adsorption to bentonite clays is needed to guide the selection, modification, and application of the clays as aflatoxin binders.

The objective of this study was to test a hypothesis that a smectite's selectivity and adsorption capacity for aflatoxin was mainly determined by the size matching requirement on interlayer surface domains and the aflatoxin molecules. Three approaches were used to vary the size of nanometer-scaled nonpolar domains in the interlayer of smectites: 1) exchanging interlayer cations, 2) selecting natural bentonites with different cation exchange capacities (CEC), and 3) reducing charge density of a high CEC smectite.

Six bentonites were fractionated, with their major mineralogical and chemical properties determined. Clay suspensions saturated with different cations were tested for aflatoxin adsorption. Some aflatoxin-smectite complexes were prepared and analyzed with FTIR and XRD. AfB₁ adsorption isotherms were fitted with Langmuir, modified Langmuir with adsorption dependent affinity, and exponential Langmuir models.

Divalent exchange cations with low hydration energy in general resulted in a much higher adsorption capacity and affinity for all six natural bentonite clays. Cations with smaller hydration radii tended to further enhance the adsorption process for aflatoxin on smectites. Charge density of smectite had shown significant effects on the adsorption capacity, affinity, and the isotherm shape. Aflatoxin adsorption isotherms on the six natural smectites and the CEC-reduced 5OK samples by Hofmann and Klemen effects suggested that there is an optimal CEC range between 80~110 cmol(+)/kg for the best aflatoxin binding smectites. When the smectite has a CEC within this range, the mineral has the highest affinity and adsorption capacity for AfB₁.

The aflatoxin adsorption results after cation exchange treatment, selection of different CEC smectites, and the CEC reduction on 5OK confirmed the importance of size and polarity matching on the nanometer scale in smectites' adsorption for AfB₁. All clay samples tested in this study were capable of adsorbing aflatoxin into interlayers, and the charge density seemed to have no effect on bonding strength.

DEDICATION

This thesis is lovingly dedicated to my awesome husband, Zhe Shi
for his unconditional love that supports me all along the way.

ACKNOWLEDGEMENTS

I would like to thank my committee chair, Dr. Deng, for the opportunity to work with him, and for his help and guidance during the research process.

I also would like to extend my sincere appreciation to my committee members, Dr. Senseman and Dr. Capareda, for their guidance and support throughout the course of this research.

Thanks also go to my friends and colleagues and the department faculty and staff for making my time at Texas A&M University a great experience.

Finally, thanks to my brothers and sisters in Christ for their encouragement and help in every aspect. Thanks to the LORD.

TABLE OF CONTENTS

	Page
ABSTRACT	ii
DEDICATION.....	iv
ACKNOWLEDGEMENTS	v
TABLE OF CONTENTS.....	vi
LIST OF FIGURES	viii
LIST OF TABLES.....	ix
1. INTRODUCTION	1
2. MINERALOGICAL EVALUATION OF SIX NATURAL BENTONITES WITH DIFFERENT CATION EXCHANGE CAPACITIES	8
2.1 Materials and Methods	8
2.1.1 Size Fractionation.....	9
2.1.2 X-ray Diffraction (XRD) Analysis.....	11
2.1.3 Scanning Electron Microscopy (SEM).....	12
2.1.4 Cation Exchange Capacity (CEC) Determination.....	12
2.2 Results and Discussion.....	14
2.2.1 Texture of Bentonites	14
2.2.2 Mineral Identification and Morphology	15
2.2.3 Cation Exchange Capacity	18
2.3 Conclusions.....	18
3. AFLATOXIN ADSORPTION ON CLAY FRACTIONS OF NATURAL BENTONITES	20
3.1 Introduction.....	20
3.2 Materials and Methods	21
3.2.1 Exchange Cation Saturation.....	21
3.2.2 Aflatoxin Adsorption Isotherms	22
3.2.3 Curve Fittings for Aflatoxin Adsorption Isotherms	23
3.2.4 Synthesis of Aflatoxin-Smectite Complexes	25
3.3 Results and Discussion.....	26
3.3.1 Aflatoxin Adsorption on 37GR Clays Saturated with Different Exchange Cations.....	30

3.3.2 Aflatoxin Adsorption on Clays with Different CEC	32
3.3.3 Characterization of Aflatoxin-Smectite Complexes.....	35
3.4 Conclusions.....	38
4. AFLATOXIN ADSORPTION ON CHARGE REDUCED SMECTITES FROM A NATURAL BENTONITE	39
4.1 Introduction.....	39
4.2 Materials and Methods	40
4.2.1 Charge Reduction	40
4.2.2 Quantification of Structural Li to Calculate Remaining CEC	41
4.3 Results and Discussion.....	42
4.4 Conclusions.....	45
5. SUMMARY.....	46
REFERENCES	48

LIST OF FIGURES

	Page
Figure 1. 1: Aflatoxin-smectite complex model proposed by Deng et al. (2010). Interlayer water molecules were not shown.	4
Figure 1. 2: Conceptual models of adsorbed aflatoxin B1 molecules (left) and the hydrated exchange cations (right) projected onto the basal siloxane surfaces of 4a by 2b smectite unit cells. The color scale bar is for the surface charge of aflatoxin molecules. The smectite cell dimension is based on Viani et al. (2002). The aflatoxin model is reproduced with the permission of Elsevier, from Deng and Szczerba (2011).	5
Figure 2. 1: X-ray diffraction patterns of clay fractions	15
Figure 2. 2: Secondary electron images of clay fractions of six bentonites.	17
Figure 3. 1: AfB1 adsorption isotherms on 37GR clay saturated with Li, Na, K, Cs, Mg, Ca, Sr and Ba, and their exponential Langmuir equation fits.	31
Figure 3. 2: AfB1 adsorption isotherms on 1MS, 7AZ, 8TX, and 16MX clays	32
Figure 3. 3: Langmuir, ELM and QKLM fits of AfB1 adsorption isotherms	33
Figure 3. 4: AfB1 adsorption capacity & affinity on clays with different CEC.	34
Figure 3. 5: Infrared spectra of aflatoxin-smectite complexes on six clays	36
Figure 3. 6: Basal spacings of 37GR clay and six aflatoxin-smectite complexes	37
Figure 4. 1: AfB1 adsorption on charge reduced 5OK clays	43
Figure 4. 2: AfB1 adsorption capacity & affinity on charge reduced 5OK clays.	44

LIST OF TABLES

	Page
Table 2. 1: Size fractions of six bentonites	14
Table 2. 2: Cation exchange capacity of clay fractions of six bentonites.	19
Table 3. 1: Adsorption isotherm fit parameters for aflatoxin adsorption on the clay fractions saturated with different cations*. (Part A).....	27
Table 3. 2 Adsorption isotherm fit parameters for aflatoxin adsorption on the clay fractions saturated with different cations*. (Part B).....	28
Table 3. 3 Adsorption isotherm fit parameters for aflatoxin adsorption on the clay fractions saturated with different cations*. (Part C).....	29

1. INTRODUCTION

Mycotoxins are secondary metabolites produced by fungi and are among the most toxic substances in existence. The major mycotoxins related to food or feed safety are aflatoxins, ochratoxins, fumonisin, zearalenone, and trichothecene. Among these naturally occurring toxins, aflatoxins have drawn the most attention due to their greatest toxicity to animals and humans. Aflatoxin exposure risk is especially high in developing countries.

Normally produced by fungi *Aspergillus flavus* and *Aspergillus parasiticus*, aflatoxins are a series of carcinogenic compounds with relatively small molecular weights (Murphy et al., 2006). Among the approximately 20 different forms of aflatoxins detected, aflatoxin B₁ is the most abundant and also the most toxic natural carcinogen known (Squire, 1981). The U.S. Food and Drug Administration still allows aflatoxins at low levels of less than 20 ug/kg in food, since occurrence of these carcinogens in grains, oil seeds and nuts is considered unavoidable. They can be produced in any stages of crop production, transportation, storage, and food or feed process.

Best management practices, such as sufficient irrigation, early harvest, and reducing humidity in storage have been proven to work effectively in preventing aflatoxin contamination (Zain, 2011). In addition to the prevention measures, various techniques have been developed to detoxify aflatoxin-contaminated food or feed.

Application of ammonium hydroxide or anhydrous ammonia can effectively reduce aflatoxin concentration in grains, nuts, as well as feed, and therefore reduce the toxicity of aflatoxins to animals such as rainbow trout (Brekke et al., 1977). It has been observed that ammonia could induce decomposition of aflatoxins starting from the ketone group in the cyclopentene ring (Grove et al., 1981), resulting in molecules with less toxicities. Nixtamalization is another method to decompose aflatoxins. This method was originally a cooking procedure for corn (Herrera et al., 1986). Due to the strong alkalinity, boiling corn kernels with lime water can soften grains before they are used in food preparation, as well as break down aflatoxins to more soluble forms that can be removed by rinsing. Even at low CaO concentrations, nixtamalization was still effective in destroying aflatoxins during tortilla preparation (Arriola et al., 1988). However, ammoniation is not approved by the U.S. Food and Drug Administration (FDA) as a detoxification method yet, probably due to the formation of uncertain toxic residues. The alteration of food flavor and nutrients also limited applications of nixtamalization.

Using clays to deactivate aflatoxins is attractive due to their broad availability, low cost, and cultural acceptance. Clay additives have long been used in animal feeds to prevent caking as well as improve pelleting (Guevara-Gonzalez, 2011). Extra benefits have been observed as these clays could reduce aflatoxin toxicity to animals from contaminated feeds. Numerous commercial clays were tested as aflatoxin binders in different animal feeds with varied conditions, and significant reductions of toxicity were observed in most of them (Phillips et al., 1988, 1995; Lindemann et al., 1993; Scheideler 1993; Schell et al., 1993; Abdel-Wahhab et al., 1999; Ellis et al., 2000; Pimpukdee et al.

2004; Bailey et al., 2006). Considering mineralogical compositions of all these clays, bentonites have drawn the most attentions due to their high binding capacities for aflatoxins.

Bentonite is defined as a rock term used to describe natural clay materials that are composed primarily of the clay mineral montmorillonite (Eisenhour and Brown, 2009). Montmorillonite is one of the smectite minerals that are classified as a group of 2:1 phyllosilicates. They consist of one octahedral sheet sandwiched by two tetrahedral silica sheets. Isomorphic substitutions in layer structures of smectites make it negatively charged naturally, and the layer charge was compensated by interlayer cations. The interlayer space of smectites is highly expandable after gaining moisture, and interlayer cations are exchangeable. All these properties could make smectites potentially good sorbents with wide applications. Montmorillonite is the most common mineral in the smectite group. Other less common smectites are beidellite, nontronite, saponite, and hectorite (Odom, 1984).

Generally speaking, smectites have been shown to be capable of adsorbing aflatoxins from aqueous solutions. Their maximum loads as well as affinity determined from adsorption isotherms, however, may vary significantly (Phillips et al., 1988). Little was known about clay properties that strongly affect the adsorption process, which limited the selection and modification of bentonites as aflatoxin amendments. Basic evaluations on major mineralogical, chemical and physical parameters of bentonites from different sources were conducted, and have been used to correlate with aflatoxin adsorption capacities to clays (Kannevischer et al., 2006; Mulder et al., 2008; Tenorio et

al., 2008). It was concluded that bentonites with high content of smectites, little organic matter, moderate layer charge, and neutral pH tend to behave better in the adsorption (Tenorio et al., 2008).

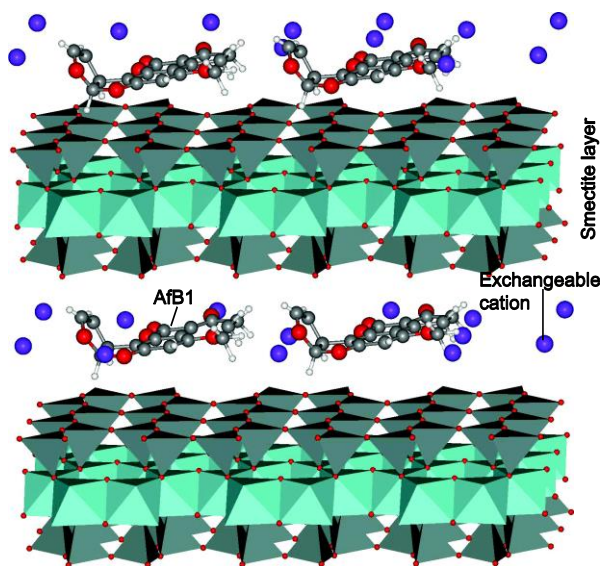


Figure 1. 1: Aflatoxin-smectite complex models proposed by Deng et al. (2010). Interlayer water molecules were not shown.

Considering binding mechanisms between aflatoxin molecules and smectites as a theoretical basis for clay selection, various methods including infrared and molecular modeling have been used in studying aflatoxin-smectite complexes. (Phillips et al., 1995; Deng et al., 2010; Deng and Szczerba, 2011). Deng et al. (2010) observed that aflatoxins could occupy interlayer spaces of smectites (Figure 1.1), interacting with different exchange cations and water. It was also hypothesized that the size and polarity matching among aflatoxins, cations and nanoscale domains on smectite surfaces was determining the stability and selectivity of adsorption. Direct ion-dipole interactions and

H bonding through water were both responsible for connecting aflatoxins and smectites, but dominated at different humidity (Deng et al., 2010).

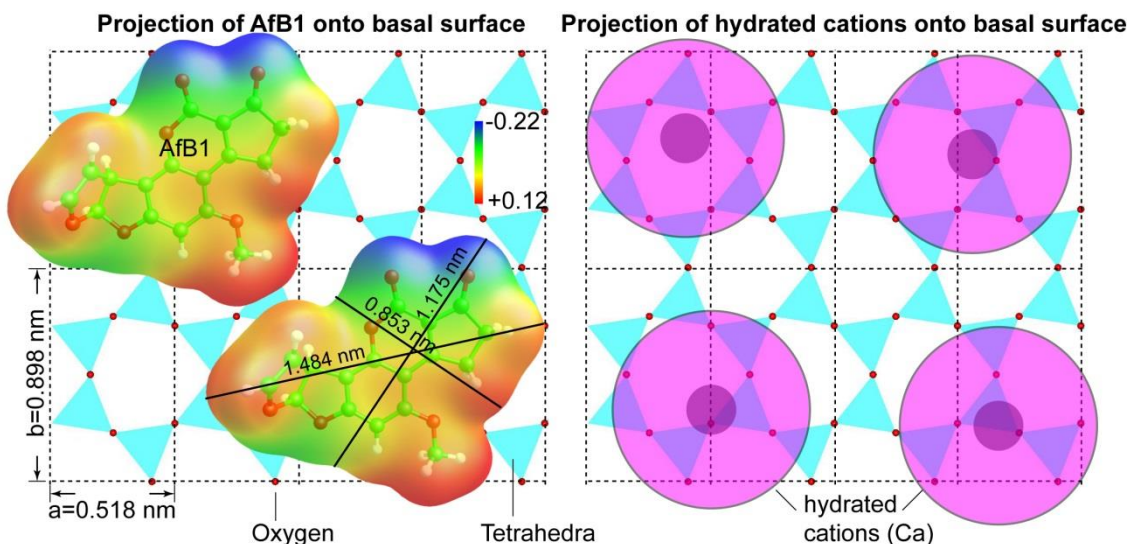


Figure 1. 2: Conceptual models of adsorbed aflatoxin B₁ molecules (left) and the hydrated exchange cations (right) projected onto the basal siloxane surfaces of 4a by 2b smectite unit cells. The color scale bar is for the surface charge of aflatoxin molecules. The smectite cell dimension is based on Viani et al. (2002). The aflatoxin model is reproduced with the permission of Elsevier, from Deng and Szczerba (2011).

The structure of an aflatoxin B₁ molecule is featured by a co-planar configuration of four rings (Figure 1.2, Left), based on computational optimization and X-ray diffraction studies (Deng and Szczerba, 2011). The projected area for this molecule was estimated at around 1.04 nm², when adsorbed onto interlayer surface of smectites. As described in the work of Grant and Phillips (1998), the horizontal cross-sectional area of an aflatoxin molecule was 0.883 nm². A single montmorillonite unit cell could give a 0.465 nm² of basal surface area (Viani et al., 2002). Therefore, each aflatoxin molecule will possibly occupy more than two unit cells (Figure 1.2, Left). The specific surface

area of smectites is about $800 \text{ m}^2/\text{g}$, including both external and internal surfaces. Assuming all interlayer surfaces of smectites were occupied by a single layer of aflatoxin B₁, the calculated aflatoxin loading would be around 0.7 mol/kg . This is in good agreement with the highest aflatoxin adsorption capacity of 0.68 mol/kg on smectites, as reported by Kannewischer et al. (2006).

Exchange cations balancing negative charges of smectites tend to occupy polar domains of basal surfaces (Figure 1.2, Right) which is due to the structural charge caused by isomorphic substitution. Meanwhile, aflatoxin molecules were more likely to occupy nonpolar domains (the unoccupied space between the exchange cations in Figure 1.2, Right.). Apparently, the valence of exchange cations, the amount of hydrated water, and the layer charge of smectites are determining the surface area of unoccupied domains on the parallelogram grid of smectites. Assuming that only one layer of aflatoxin molecules would fit into these remaining domains among hydrated exchange cations, the maximum aflatoxin loadings were highly related to the size matching. Basing on the estimation above, divalent cation saturations for smectites might introduce greater unoccupied surface areas for aflatoxins, in comparison with monovalent cation saturations.

The objective of this study was to test the hypothesis that a smectite's selectivity and adsorption capacity for aflatoxin was mainly determined by the size matching requirement on interlayer surface domains and the aflatoxin molecules. Three approaches were used to vary the size of nanometer-scaled nonpolar domains in the interlayer of smectites: 1) exchanging interlayer cations, 2) selecting natural smectites

with different cation exchange capacity (CEC), and 3) reducing charge density of a high CEC smectite.

Based on previous studies and preliminary tests (Kannevischer et al., 2006) on their aflatoxin adsorptions, six bentonites with varied cation exchange capacities were chosen to test this hypothesis. Before modification of smectites separated from these bentonites, mineral compositions and chemical properties were analyzed to check smectites' purity and potential effects of other minerals in the clays on aflatoxin adsorption. Their abilities to extract aflatoxins from dilute aqueous solutions were quantified with adsorption isotherms. One of these bentonite samples with relatively high CEC and low aflatoxin adsorption was selected for charge reduction experiments, according to the Hofmann & Klemen effects. All these procedures worked together in giving a detailed view about bentonites as aflatoxin binders, where varied performances were observed and possible explanations were presented.

2. MINERALOGICAL EVALUATION OF SIX NATURAL BENTONITES WITH DIFFERENT CATION EXCHANGE CAPACITIES *

2.1 Materials and Methods

Six bentonites analyzed in this study were referred to as 1MS, 5OK, 7AZ, 8TX, 16MX and 37GR. They were coded according to their origins: Mississippi, Oklahoma, Arizona, Texas, Mexico, and Greece, respectively. They all showed high content of smectite in previous tests (Mulder et al., 2008; Tenorio et al., 2008), which made them suitable for aflatoxin adsorption. A great difference in layer charge density among these six samples may lead to different aflatoxin adsorption. This difference also served as a point of interest within the group.

The six bentonite samples had been air-dried, ground, and then passed through 2-mm sieves. Moisture content was measured on weight differences before and after overnight drying the samples at 105 °C. These values were later used to calculate the oven-dried weight of the samples used in size fractionation. For each bentonite, approximately five grams of air-dried sample was weighed into a 250-mL centrifuge bottle and deionized water was added into the bottle to obtain a 5:1 water:clay ratio. Bottles were capped and shaken for 30 min on a reciprocation shaker, then centrifuged at 2,000 rpm (1,070 g) for 10 min, or until the supernatant became clear. The supernatant was siphoned off and the sediments were left in centrifuge bottles for further treatments.

* Part of the data reported in this chapter is reprinted with permission from “The determinative role of the exchange cation and layer-charge density of smectite on aflatoxin adsorption” by Deng, Y., Liu, L., Barrientos Velzaquiz, A. L., and Dixon, J. B., 2012. *Clays and Clay Minerals*, 60(4), 374-386, Copyright [2012] by The Clay Minerals Society.

The procedures described in the Soil Mineralogy Lab Manual (Deng et al., 2009) were followed in this study. Flocculating and cementing materials in samples were removed to enhance the dispersion of individual mineral particles. Fifty mL of pH 5 sodium acetate buffer solution was added to each sample in the 250-mL centrifuge bottles to remove carbonate minerals. After particles were dispersed in the solution by shaking, the bottles were placed in a pre-heated water bath of 90 °C for about 30 min. Then bottles were centrifuged at 2,000 rpm (1,070 g) for 5 min, and the supernatant was siphoned off. Above procedures were repeated till CO₂ bubbling ceased from samples when heated. As bentonites contained little organic matter, the procedures to remove organic matter were omitted for these samples.

2.1.1 Size Fractionation

Samples in centrifuge bottles were washed with deionized water to remove chemical residuals and then suspended in 50 mL of diluted pH 10 Na₂CO₃ solution. Particle dispersion was accomplished by repeatedly adding 50 mL of pH 10 Na₂CO₃ solution, shaking, and centrifuging at 2,000 rpm (1,070 g) for 10 min, and clear supernatant was siphoned off. The Na₂CO₃ treatment was repeated until supernatant became cloudy after centrifugation, which indicated large aggregates breaking down and good dispersion of particles in suspension.

Sand particles were separated by sieving the suspensions with a 53-μm sieve inside a funnel. All suspensions in centrifuge bottles were transferred onto the sieve and passed through it. The sieve was flushed with pH 10 Na₂CO₃ solution when clogged. Sand particles remaining on the sieve were rinsed by deionized water and transferred to

aluminum dishes. Sands were then oven dried at 105 °C overnight, cooled to room temperature and weighed.

Silt and clay fractions were collected as cloudy suspensions in large beakers below the funnel. Clay particles were separated from silt particles by centrifugation based on Stokes' Law. The suspension of each sample was transferred into two 250-mL centrifuge bottles for further dispersion, with approximately 200 mL of pH 10 Na₂CO₃ solution added into each bottle. Then sediments were shaken up by hand, and bottles were centrifuged at 750 rpm (150 g) for 3.2 min when particles with size equivalent to >2 µm spherical quartz diameter could settle at the bottoms. Upper suspensions which contained only < 2 µm clay were siphoned to 4,000-mL plastic beakers, one for each sample. The procedures were repeated until the upper portions became clear, while care was taken to avoid breaking down silt particles. Remaining particles in centrifuge bottles were mostly 2- to 53- µm silts or silt-sized aggregates. They were kept in bottles as suspensions and weighed. Sub-samples of silt particles were taken and oven dried at 105 °C to calculate silt contents.

Large volumes of clay suspensions were collected in 4,000-mL beakers during the separation. About 50 g of NaCl powder was added to each beaker, and left overnight to flocculate the clays. Clear supernatant was discarded while clay aggregates settled down at bottom. These clay-water mixtures were then centrifuged at 1,000 rpm (268 g) for 5 to 15 min, and supernatant was discarded to further reduce the volume. Extra salts were removed by dialyzing condensed clay suspensions against deionized water. All clay suspensions were transferred into dialysis tubing and fully immersed in deionized

water in 4,000-mL beakers. Water in beakers was changed every two hours and suspensions in tubing were agitated frequently. Dialysis was considered complete when the electronic conductivity of bath water was lower than 5 $\mu\text{S}/\text{cm}$. Clay suspensions were then transferred into 250-mL centrifuge bottles. The contents of clays were quantified gravimetrically after drying 3 mL of suspensions at 105 °C. Total mass of harvested clay from each bentonite was calculated based on the weight of suspension and clay content.

Clay fractions, collected as stable suspensions, were used for further treatments and studies. They were homogeneous and easy to handle, as well as relatively simple to analyze when comparing with bulk samples in powders.

2.1.2 X-ray Diffraction (XRD) Analysis

XRD analyses were conducted to check mineral compositions of clay, silt, and sand fractions of each bentonite. Clay fractions collected as suspensions were saturated with Mg^{2+} to facilitate identification of phyllosilicates, as their d-spacings can vary depending on interlayer cation composition, charge density, and solvent. For each sample, about 3 mL of suspension containing 50 mg of clay was transferred into a 50-mL centrifuge tube, and 0.5 M MgCl_2 solution was added to the 15-mL mark of the tube to replace exchange cations on clays with Mg^{2+} . Tubes were shaken for 20 minutes, and centrifuged for 10 mins at 2,000 rpm (1160 g). Upper clear solutions were discarded with care. Clays were washed with MgCl_2 solution as described above for two more times to ensure that clays were fully saturated by Mg^{2+} , then washed by deionized water for two times. A decreasing amount of water (10 mL and then 5 mL) was used in the

sequential washing to avoid dispersing the clays into diluted suspensions. Finally, clays were suspended in about 1 mL of deionized water after the last washing.

Appropriate amounts of suspensions were transferred onto one-inch-diameter glass discs and air dried under a watch glass. These glass discs with clay samples were analyzed with XRD, then misted with a 20% glycerol solution and analyzed again to check basal spacing expansion of smectites in clays. X-ray diffraction patterns of these translucent samples were recorded on a BRUKER D8 ADVANCE diffractometer (Bruker Austria GmbH, A-1230 Wien, Austria) with Cu K α radiation.

2.1.3 Scanning Electron Microscopy (SEM)

A QUANTA 600F field emission scanning electron microscope (FEI, Hillsboro, Oregon, USA) equipped with X-ray energy dispersive spectrum detector was used to examine the morphology of clays and their chemical compositions. Clay particles of six bentonites were fixed onto SEM stubs using conductive tabs. A small portion of each well-dispersed clay suspension was diluted and only a few drops were pipetted onto SEM stubs, air dried and then dried under an infrared heating lamp.

2.1.4 Cation Exchange Capacity (CEC) Determination

Cation exchange capacity (CEC) is a measure of the quantity of readily exchangeable cations balancing the negative charge on structures of minerals or organic matter. In total, twelve 50-mL centrifuge tubes were labeled and weighed before use. For each sample, an adequate amount of clay suspension was weighed in duplicate,

containing approximately 100 mg of clay into two centrifuge tubes. Weights of all twelve tubes with clays were then recorded.

Clays in centrifuge tubes were washed with 0.5 M CaCl_2 solution three times to saturate exchange sites with Ca^{2+} . For each washing, 20 mL of solution was added into each tube. Then all tubes were shaken for 15 mins and centrifuged at 1,500 rpm (650 g) for 10 mins. Supernatants were discarded during the washing. The high concentration of CaCl_2 caused complete cation exchange by keeping a low replaced cation:Ca ratio in the solution. After that, clays were washed with 0.005 M CaCl_2 solution three times to bring the Ca concentration in the residue solution to a known value (0.005 M), and to avoid possible clay loss due to dispersion if water was used in the washing. The low concentration of CaCl_2 was used to permit weighing the interstitial solution to determine volume. After Ca saturation, the weights of tubes with clay and interstitial solution were recorded.

Lastly, these Ca-saturated clays were washed with 15 mL of 0.5 M MgCl_2 four times to release adsorbed Ca^{2+} . A 100-mL volumetric flask was used to combine all clear supernatants collected during the washing for each sample. The solution was brought up to the 100-mL volume with the 0.5 M MgCl_2 used above after the last washing, and then mixed thoroughly. After that, 20.00 mL of this solution was quantitatively transferred into another 100-mL volumetric flask to make a 5-fold dilution with DI water. About 20 mL subsample of this diluted solution was taken out and stored in a 20-mL plastic vial for atomic absorption analysis of Ca. The vials were capped and kept in a refrigerator to prevent microbial growth.

The weights of clay residues in centrifuge tubes were determined. Excess MgCl_2 in clay residues was removed by another washing with 15 mL of distilled water. The tubes with clay residues were dried at 60 °C in an oven before they were weighed. All calculations for CEC measurements were based on weights and Ca concentrations.

2.2 Results and Discussion

2.2.1 Texture of Bentonites

All six bentonites contained abundant clay but little sand (Table 2.1). They were identified as clays in texture based on the soil texture triangle. The sand content was slightly higher in samples 1MS and 5OK, compared with the other four bentonites. As for sample 16MX, a silt content of almost 40% made it less clayey. As particle size or surface area could affect adsorption, these differences must be eliminated by applying only clay fractions to aflatoxins.

Table 2. 1: Size fractions (% wt) of six bentonites

	1MS	5OK	7AZ	8TX	16MX	37GR
Origin	Mississippi	Oklahoma	Arizona	Texas	Mexico	Greece
Sand	8.64	5.72	0.69	2.79	0.40	0.16
Silt	16.25	7.19	6.59	6.46	39.50	24.16
Clay	75.11	87.09	92.71	90.76	60.10	75.68

2.2.2 Mineral Identification and Morphology

When a Mg-saturated clay is solvated with glycerol, a peak with d-spacing of 1.8 nm on the X-ray diffraction pattern is a good indication of the presence of mineral smectite in the clay.

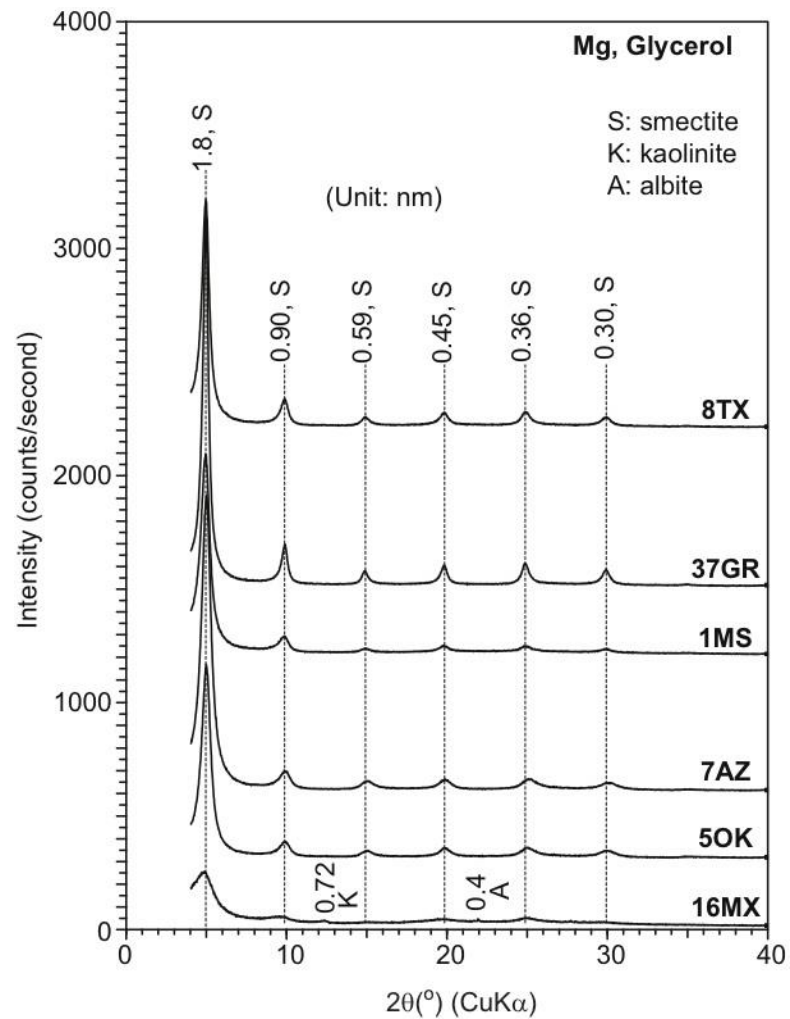


Figure 2. 1: X-ray diffraction patterns of clay fractions saturated with Mg and solvated with glycerol.

According to Figure 2.1, smectites were the only or dominant mineral in clay fractions of all six bentonites. No other clay minerals were identified in samples 1MS, 5OK, 7AZ, 8TX or 37GR on the XRD patterns. Appreciable kaolinite and albite peaks were detected in the clay fraction of 16MX. These impurities tend to affect chemical or mineralogical properties of sample 16MX, which may alter its ability to adsorb aflatoxin.

During the analysis of scanning electron microscopy, minerals detected with XRD were main targets that have been searched for. Numerous secondary electron images were recorded for each clay on SEM to give a general view of the morphology of these clay minerals. Representative images of six clays were selected and shown in Figure 2.2.

In these images, aggregates with light color and rose-like flakes were identified as smectites. Although the size of smectite particles was usually very small, the aggregation may form large particles in the size of silt. A trace amount of halloysite was found in sample 8TX, while the low quantity made it undetectable with XRD. Kaolinite and albite were not identified with SEM in this set of samples.

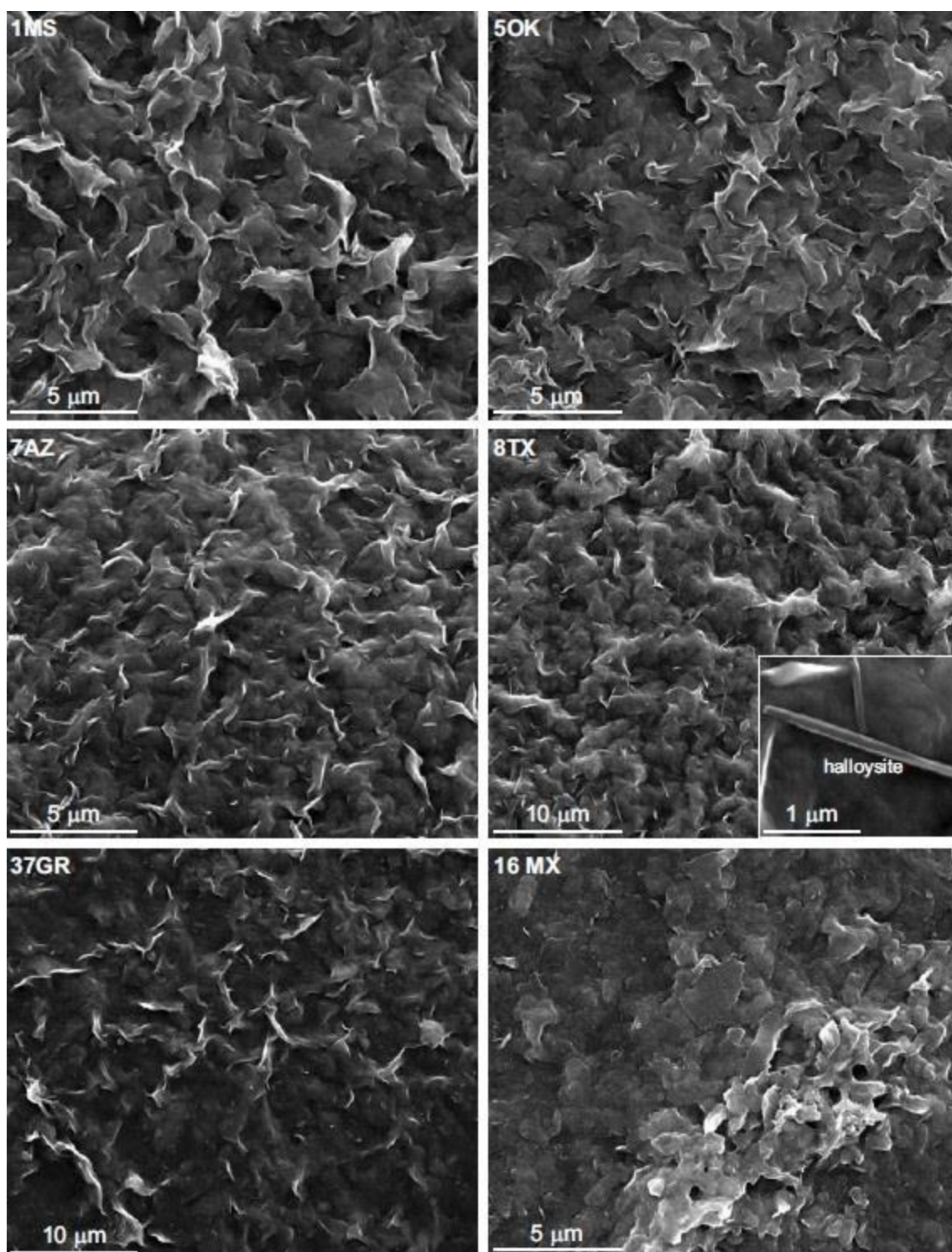


Figure 2. 2: Secondary electron images of clay fractions of six bentonites.

2.2.3 Cation Exchange Capacity

The results of cation exchange capacity determination of clay fractions, combined with identified clay minerals in six bentonites were shown in Table 2.2. It was noticeable that samples 5OK and 7AZ had much higher CEC than other samples. Three samples with moderate CEC of around 100 cmol/kg were 1MS, 8TX and 37GR. Due to the simple mineral composition of these five samples, CEC of clay fractions were all attributed to smectites. The sample with the lowest CEC was 16MX. However due to the presence of kaolinite and albite in 16MX, it was not possible to make an estimation of smectitic CEC in this sample.

Table 2. 2: Cation exchange capacity of clay fractions of six bentonites.

Sample	CEC (cmol/kg)	Minerals Identified
1MS	107.7	Smectite
5OK	136.6	Smectite
7AZ	138.4	Smectite
8TX	94.6	Smectite, trace halloysite
16MX	78.1	Smectite, kaolinite, albite
37GR	111.5	Smectite

2.3 Conclusions

Six bentonites analyzed in this study were all classified as clay, due to their high contents of clay fractions. Smectite was identified as the dominant mineral in clay

fractions of all six samples, while sample 16MX also contained impurities of kaolinite and albite. According to differences in CEC values of clays, these six samples could be classified into three groups: two samples with high CEC (5OK, 7AZ), three with moderate CEC (1MS, 8TX, 37GR) and one sample with low CEC (16MX).

3. AFLATOXIN ADSORPTION ON CLAY FRACTIONS OF NATURAL BENTONITES *

3.1 Introduction

Previous studies indicated that aflatoxin molecules could actually occupy the interlayer spaces of smectite, while exchange cations and water were also involved in the bonding of aflatoxin to smectite (Deng et al., 2010; Deng and Szczerba, 2011). These observations have led us to formulate the hypothesis that size and polarity matching between adsorbed aflatoxin molecules and their adsorbing domains on the nanometer scale can determine the adsorption process. We further hypothesized that high aflatoxin adsorption capacity and selectivity can be achieved when a smectite's surface polarity and interlayer environments are modified to optimize the matching requirements.

The objective of this part of study was to investigate the mechanisms behind aflatoxin adsorption on smectites, including influences of altered interlayer exchange cations as well as charge densities of minerals.

In this case, eight cations with differences in valence and hydration energy were chosen to saturate the clay, and to alter the interlayer environment of smectites.

Adsorption of aflatoxin B₁ on clay fractions of six natural bentonites was investigated after exchange cation saturation. The effectiveness of clays was evaluated by fitting

* Reprinted with permission from “The determinative role of the exchange cation and layer-charge density of smectite on aflatoxin adsorption” by Deng, Y., Liu, L., Barrientos Velzaquiz, A. L., and Dixon, J. B., 2012. *Clays and Clay Minerals*, 60(4), 374-386, Copyright [2012] by The Clay Minerals Society.

adsorption isotherms with Langmuir, exponential Langmuir, and modified Langmuir with adsorption dependent affinity models. An X-ray diffraction and infrared spectroscopy analyses of synthesized aflatoxin-smectite complexes were also conducted to elucidate the binding mechanisms.

The high content of almost pure smectite in bentonite 37GR made it ideal to be tested as a model in the first trial. Eight cations were applied on 37GR clay, and then two of them were selected to be tested on the other five samples. These natural clays with variable charge densities also behaved differently in adsorption, and a brief correlation between cation exchange capacity and efficiency of aflatoxin adsorption was observed in this study. In lack of a natural smectite sample with a high purity and a low charge density, this correlation was still one step away from perfection. The study described in Chapter 4 will be focused on supplemental experiment designs and results as verification.

3.2 Materials and Methods

3.2.1 Exchange Cation Saturation

Clay fractions of six bentonites were saturated with Na during dispersion and size fractionation. To investigate the effect of exchange cations on aflatoxin adsorption, seven cations, Li, K, Cs, Mg, Ca, Sr, and Ba were selected to replace Na in interlayers of smectites. Chloride solutions of these seven cations were prepared for the cation saturation treatments. Concentrations of monovalent cations of these chloride solutions were 1 M, and of divalent cations were 0.5 M. The procedure for cation saturation was the same as the cation exchange procedure described in section 2.1.2 except the type of

cations used. Fifty mg of clay was used in each cation saturation. Clay content in final suspensions was calculated based on weights of the clay and suspension.

Based on aflatoxin adsorption capacities of 37GR clays saturated with Li, Na, K, Cs, Mg, Ca, Sr, and Ba, two cations, Ca, Ba, which induced great aflatoxin adsorption, were selected to saturate the other five smectite samples. Selecting Ca saturation was due to the fact that Ca is a common exchange cation in natural bentonites. Selecting Ba saturation was due to its greatest improvement on aflatoxin adsorption as demonstrated on sample 37GR.

Aliquots of different cation modified clays were diluted with deionized water to obtain 5-mL suspensions with a clay content of 2 mg/mL. Weights of suspensions before and after the dilution were recorded to calculate exact clay content. These stock and diluted clay suspensions were kept in a refrigerator at 4 °C.

3.2.2 Aflatoxin Adsorption Isotherms

Aflatoxin adsorptions on clays were measured following the procedure described by Kannewischer et al. (2006). Fifty mg of aflatoxin B₁ (AfB₁) powders (Sigma-Aldrich) was dissolved into an adequate amount of acetonitrile solvent to make a 1,000 ppm (µg/mL) AfB₁ stock solution. A fresh 8 ppm (µg/mL) AfB₁ working solution was prepared by diluting the stock solution with deionized water. Diluted aflatoxin solutions seemed perishable and therefore, one fresh working solution was prepared for each set of isotherms.

By mixing deionized water and the 8 ppm (µg/mL) AfB₁ working solution according to desired volume ratios, three sets of aflatoxin solutions with concentrations

of 0.0, 0.4, 1.6, 3.2, 4.8, 6.4, and 8.0 ppm ($\mu\text{g/mL}$) were obtained. A pipette was used to transfer water and the working solution to 15-mL centrifuge tubes. The final volume of mixture in each tube was 5.0 mL. One set of the solutions were used as standards in aflatoxin quantification. For the other two sets of aflatoxin solutions, an appropriate amount (approximately 0.05 mL) of 2 mg/mL clay suspensions, containing 0.100 mg of clay, was added into each tube. In most cases, two duplicates of a total fourteen tubes were used for one isotherm.

Tubes for standards and samples were prepared simultaneously, followed by over-night shaking on a rotary shaker at 200 motions/min. After the adsorption reached equilibrium, these tubes were centrifuged at 4,500 rpm (5,100 g) for 57 min. Concentrations of aflatoxin left in supernatants were quantified with a Beckman Coulter DU 800 UV-Visible spectrophotometer. The peak position of absorbance was found at 363 nm for AfB₁ in water, and it was used throughout the whole study. The molar absorbance coefficient value was 19,378 as measured in previous studies. Aflatoxin concentrations for both standards and samples were calculated on the basis of absorbance.

3.2.3 Curve Fittings for Aflatoxin Adsorption Isotherms

Amounts of aflatoxin adsorbed on clays (mol/kg) were calculated based on AfB₁ concentration differences between solutions with and without adsorption, as well as quantity of clays. Most adsorption isotherms could be fitted well with the Langmuir equation, while some isotherms showed an S-shape and could not. In this case, two modified Langmuir models were introduced in this study to achieve a better fit for these

isotherms and to extract the adsorption capacity and affinity constants. Equations for all three models were

Langmuir equation:

$$q = Q_{max} \left(\frac{KC}{1 + KC} \right)$$

Exponential Langmuir equation:

$$q = Q_{max} \left(\frac{KC^n}{1 + KC^n} \right)$$

Modified Langmuir equation with q dependent affinity (QKLM):

$$q = Q_{max} \left[\frac{Ke^{(-2bq)}C}{1 + Ke^{(-2bq)}C} \right]$$

In these original or modified Langmuir equations, q is the amount of aflatoxin adsorbed on the clay; Q_{max} is the maximum adsorption capacity; C is the equilibrium concentration of aflatoxin in solution; K is the Langmuir equilibrium constant, which reflects the affinity of the clay surface for AfB₁; n is an exponential parameter meaning that there are n types of adsorption sites on or in the smectite; and b is an energy-dependent affinity parameter. Among these parameters Q_{max} and K are the most important in describing the effectiveness of adsorption. The add-in program Solver in Microsoft Excel was used to refine these parameters and to minimize the differences between measured and fitted adsorption values, on the basis of nonlinear least square regression.

3.2.4 Synthesis of Aflatoxin-Smectite Complexes

As will be seen from aflatoxin adsorption isotherms, all clays with Ba saturation adsorbed more aflatoxins. For this reason, Ba-saturated clays were chosen to synthesis aflatoxin-smectite complexes for X-ray diffraction and infrared spectroscopy analyses. The amount of Ba clay used for synthesis was 1 mg to ensure that there were enough materials. Ba-saturated clays of six bentonites were mixed with 35 mL of 8 ppm AfB₁ working solution in 40-mL centrifuge tubes. These tubes were shaken overnight to reach equilibrium, and then centrifuged at 4,500 rpm (5,100 g) for 2 hours. Supernatants were collected to quantify aflatoxin concentrations. Then 30 mL of fresh 8 ppm ($\mu\text{g/mL}$) AfB₁ working solution were added into each tube for another bout of aflatoxin treatment. Aflatoxin in the supernatant was also quantified with the UV-Visible spectrometer. Amounts of aflatoxin in complexes were calculated based on aflatoxin concentrations before and after adsorption. Resulting aflatoxin-clay complexes were washed with deionized water two times after being transferred into 15-mL centrifuge tubes. The suspension of each aflatoxin-smectite complex was transferred onto a ZnS infrared window (ClearTran, International Crystal Labs, Garfield, New Jersey, USA), air-dried, and then mounted in a dewar accessory (model DER-P11-3, Harrick Scientific Products, Inc. Pleasantville, NY, USA). Spectra were recorded on a Perkin Elmer Spectrum 100 Fourier Transform-Infrared Spectrometer (Perkin Elmer, Massachusetts, USA) at 0% humidity and 100% humidity. The nearly 0% humidity was obtained by purging the dewar with N₂ gas and the nearly 100% humidity was achieved by leaving a wet Kimwipe tissue inside the dewar accessory.

These clays were then re-dispersed in water for variable temperature X-ray diffraction analyses. After air dried on silicon plates, samples were placed in a reactor chamber XPK 900 (Anton Paar Gmbh, Graz, Austria) and analyzed with a Bruker D8 Advance X-ray diffractometer at desired temperatures. The XRD patterns of 37GR Ba clay at elevated temperatures were also recorded to monitor the collapse of smectite without adsorbed aflatoxin.

3.3 Results and Discussion

Both interlayer exchange cations and layer charge of smectites showed significant effects on the adsorption of aflatoxin B₁. Fit parameters of three Langmuir models are shown in Table 3.1, Table 3.2, and Table 3.3, with standard errors estimated with the program R. Details concerning the calculation process were described right after the tables.

The exponential Langmuir model resulted in good fits for most adsorption isotherms, which was selected for use in all following figures and discussions within this chapter.

Table 3. 1: Adsorption isotherm fit parameters for aflatoxin adsorption on the clay fractions saturated with different cations*. (Part A)

Sample	Exchange Cation	Langmuir		
		Q_{max} (mol kg ⁻¹)	K ((μM) ⁻¹)	η^2
37GR	Li	0.497±0.388	0.018±0.019	0.889
	Na	27.3**	0.0004**	0.978
	K	0.632±0.023	0.129±0.011	0.995
	Cs	0.378±0.038	0.088±0.020	0.972
	Mg	0.516±0.021	0.280±0.038	0.983
	Ca	0.595±0.034	0.351±0.064	0.968
	Sr	0.713±0.055	0.143±0.027	0.975
	Ba	0.718±0.029	0.395±0.049	0.985
1MS	Ca	0.636±0.015	0.448±0.041	0.993
	Ba	0.692±0.017	0.826±0.093	0.990
8TX	Ca	0.627±0.021	0.547±0.074	0.982
	Ba	0.662±0.022	0.868±0.123	0.978
7AZ	Ca	1.09±0.57	0.009±0.006	0.985
	Ba	0.983±0.207	0.033±0.010	0.981
5OK	Ca	27.1**	0.0004**	0.955
	Ba	0.840±0.215	0.044±0.018	0.953
16MX	Ca	0.246±0.013	0.109±0.014	0.988
	Ba	0.308±0.017	0.138±0.021	0.982

Table 3. 2 Adsorption isotherm fit parameters for aflatoxin adsorption on the clay fractions saturated with different cations*. (Part B)

Sample	Exchange Cation	Exponential Langmuir			
		Q_{max} (mol kg ⁻¹)	K ((μM) ⁻¹)	n	η^2
37GR	Li	0.202±0.092	0.0105±0.015	1.75±0.87	0.900
	Na	5.802**	0.001**	1.215**	0.988
	K	0.668±0.078	0.128±0.012	0.946±0.097	0.995
	Cs	11.6**	0.004**	0.525**	0.986
	Mg	0.505±0.046	0.280±0.040	1.04±0.17	0.983
	Ca	0.509±0.024	0.322±0.049	1.53±0.21	0.984
	Sr	0.550±0.033	0.110±0.022	1.53±0.20	0.989
	Ba	0.638±0.029	0.423±0.042	1.288±0.134	0.991
1MS	Ca	0.632±0.033	0.450±0.046	1.012±0.099	0.993
	Ba	0.700±0.036	0.804±0.119	0.971±0.108	0.990
8TX	Ca	0.600±0.033	0.577±0.084	1.12±0.15	0.984
	Ba	0.618±0.022	1.038±0.159	1.29±0.17	0.984
7AZ	Ca	0.256±0.020	0.008±0.002	1.85±0.16	0.997
	Ba	0.451±0.024	0.022±0.004	1.79±0.14	0.997
5OK	Ca	0.239±0.012	0.0008±0.0005	2.89±0.27	0.996
	Ba	0.386±0.010	0.008±0.002	2.61±0.19	0.996
16MX	Ca	0.220±0.022	0.103±0.016	1.149±0.157	0.990
	Ba	0.276±0.028	0.133±0.024	1.166±0.187	0.984

Table 3. 3 Adsorption isotherm fit parameters for aflatoxin adsorption on the clay fractions saturated with different cations*. (Part C)

Sample	Exchange Cation	Modified Langmuir with q dependent affinity			
		Q_{max} (mol kg ⁻¹)	K ((μM) ⁻¹)	b	η^2
37GR	Li	0.198±0.057	0.021±0.005	6.39±4.14	0.974
	Na	0.383±0.079	0.0176±0.002	-2.97±0.90	0.996
	K	0.593±0.057	0.127±0.012	-0.27±0.42	0.995
	Cs	0.356±0.124	0.088±0.020	-0.36±2.13	0.972
	Mg	0.478±0.029	0.224±0.054	-0.81±0.68	0.986
	Ca	0.517±0.021	0.201±0.044	-1.61±0.52	0.989
	Sr	0.549±0.022	0.096±0.014	-1.64±0.38	0.994
	Ba	0.634±0.021	0.275±0.040	-0.99±0.29	0.994
1MS	Ca	0.629±0.030	0.435±0.071	-0.09±0.36	0.993
	Ba	0.693±0.030	0.832±0.173	0.02±0.37	0.990
8TX	Ca	0.589±0.026	0.423±0.104	-0.70±0.50	0.986
	Ba	0.619±0.017	0.536±0.124	-1.06±0.41	0.989
7AZ	Ca	0.237±0.009	0.025±0.001	-4.89±0.48	0.999
	Ba	0.440±0.023	0.040±0.004	-2.52±0.45	0.996
5OK	Ca	0.237±0.012	0.017±0.003	-6.92±1.01	0.996
	Ba	0.405±0.098	0.034±0.004	-3.59±0.33	0.998
16MX	Ca	0.213±0.019	0.0970±0.017	-1.93±1.49	0.991
	Ba	0.268±0.023	0.117±0.028	-1.71±1.41	0.986

* Parameters Q_{max} , K , n , and b are reported as estimated value \pm standard error.

The model parameters were estimated with program Solver in MS Excel and program R, whereas the standard errors were estimated with program R. In most cases, program R and Solver yielded the same estimated values for the parameters.

**In a few cases whereas the adsorption data points were too far away from the L-shape, program R yielded much poorer fitting curves than Solver and therefore the parameters estimated by Solver were reported here but the standard errors were not calculated.

3.3.1 Aflatoxin Adsorption on 37GR Clays Saturated with Different Exchange Cations

Clay fractions of 37GR saturated with eight cations showed similar trends in aflatoxin B₁ adsorption isotherms. Exchange cations with different valence and size played an important role in altering the affinity and adsorption capacity of smectites for aflatoxin, as well as isotherm shapes. The exponential Langmuir equation in general fit adsorption isotherms better than the other two models. Results with fitted curves were shown in Figure 3.1:

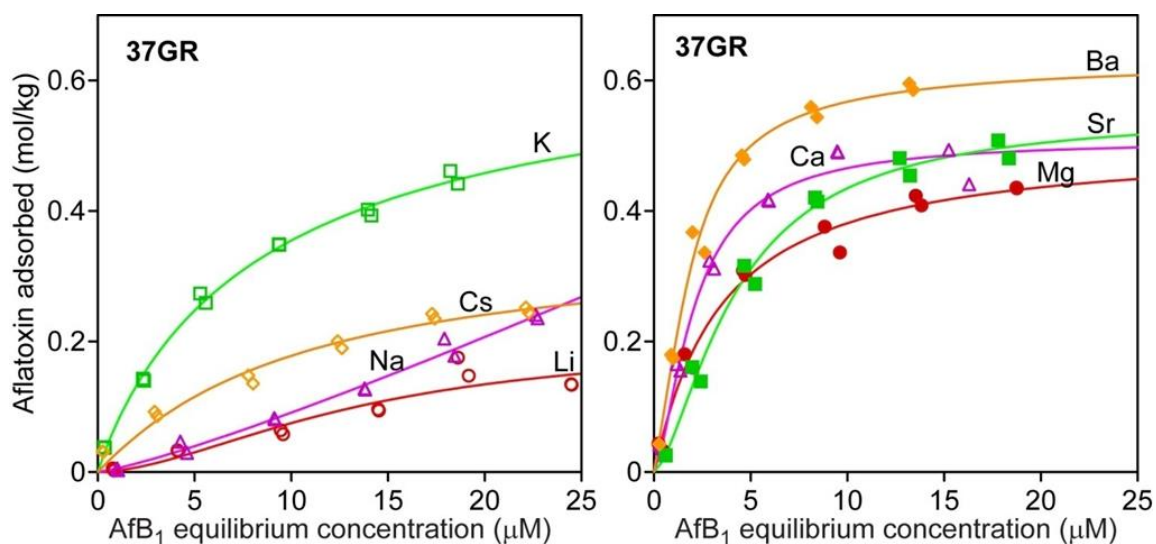


Figure 3. 1: AfB₁ adsorption isotherms on 37GR clay saturated with Li, Na, K, Cs, Mg, Ca, Sr and Ba, and their exponential Langmuir equation fits.

The divalent cation saturation in general resulted in much greater adsorption capacity and affinity of 37GR clay for aflatoxin B₁, which was in agreement with predictions discussed in Chapter 1. For either monovalent cations or divalent cations, those cations with smaller hydration radii appeared to enhance both the affinity and adsorption capacity of the clay for aflatoxin, while exceptions were observed on Cs and Sr. One possible explanation was that the large dehydrated size of these two cations would induce a much weaker interaction between cations and aflatoxin molecules.

Ba saturation was found to introduce the highest affinity and capacity of 37GR clay for aflatoxins, whereas Li saturation resulted in a most reduced adsorption. Cations leading to low adsorptions such as Li and Na also had a noticeable influence on isotherm shapes, which made their fittings with the original Langmuir equation quite poor.

3.3.2 Aflatoxin Adsorption on Clays with Different CEC

The layer charge density also showed significant effects on the adsorption process of aflatoxin on smectite. Adsorption isotherms on four clays 1MS, 7AZ, 8TX, and 16MX with Ca and Ba saturation, as well as their exponential Langmuir equation fits were shown in Figure 3.2.

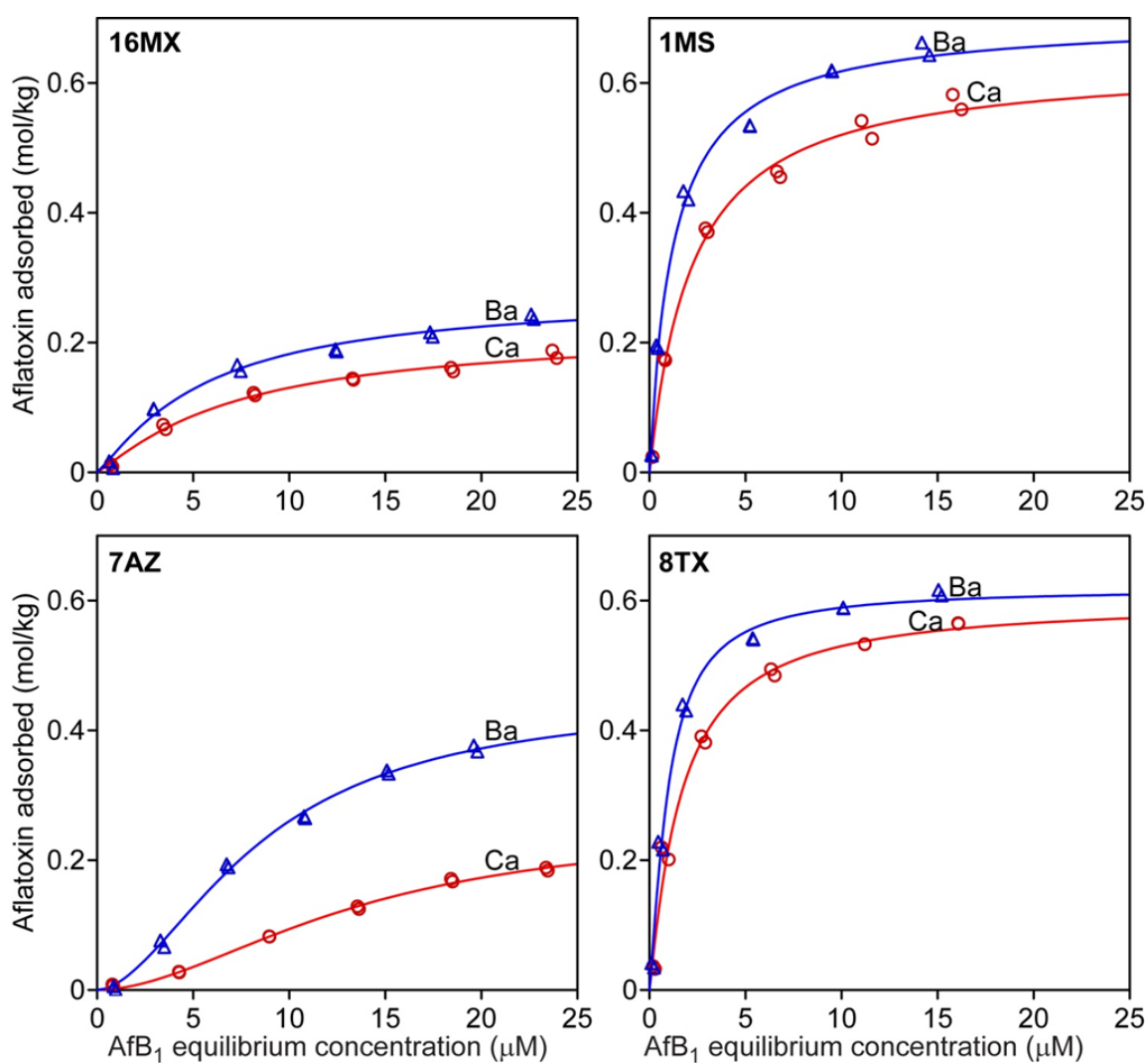


Figure 3. 2: AfB₁ adsorption isotherms on 1MS, 7AZ, 8TX, and 16MX clays saturated with Ca and Ba, and their exponential Langmuir equation fits.

Two samples with relative high CEC and low aflatoxin B₁ adsorption were 5OK clay and 7AZ clay. Their isotherm curves looked more like S-shape and would be poorly fitted with the standard Langmuir equation. Adsorption isotherms of 5OK clays fitted with all three models were plotted in Figure 3.3 as an example.

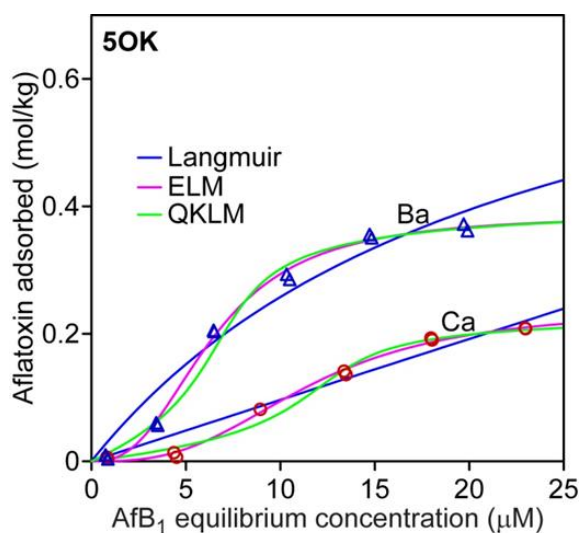


Figure 3. 3: Langmuir, ELM and QKLM fits of AfB₁ adsorption isotherms on 5OK clay saturated with Ca and Ba.

For all six clays, Ba saturation enhanced the size and polarity matching among clay particles, AfB₁ molecules and cations, therefore increased the adsorption when compared with Ca saturation. A greater increment in adsorption capacity was observed on 5OK clays and 7AZ clays, which suggested that samples with higher CEC were more sensitive to different exchange cations.

Samples with high adsorption capacity and affinity for aflatoxin were 1MS, 8TX and 37GR, and their adsorption isotherms generally could be fitted well with the Langmuir equation. While for sample 5OK and 7AZ, their low affinity for aflatoxin suggested that there was a high energy barrier for aflatoxin molecules to access the interlayer surfaces of smectites, especially when aflatoxin concentration was low. A moderate adsorption capacity and affinity for aflatoxin was observed on sample 16MX.

Figure 3.4 shows the correlations between cation exchange capacity of smectites and their aflatoxin adsorption capacity and affinity. The general trend indicated that an adequate CEC (around 110 cmol/kg) was crucial for interactions among clay particles, aflatoxin molecules and exchange cations.

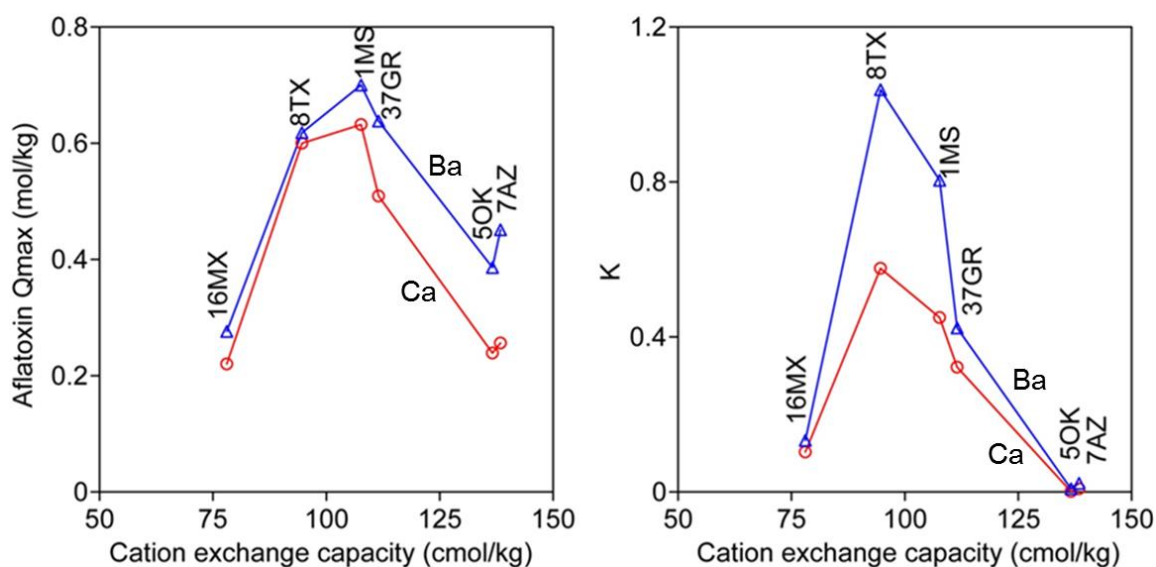


Figure 3. 4: AfB1 adsorption capacity & affinity on clays with different CEC.

Considering the presence of kaolinite and feldspars in sample 16MX, the relatively low cation exchange capacity could not be used to estimate the charge density

of the smectite in this sample. In this case, sample 16MX failed to be a very good representative for smectites with low CEC in reacting with aflatoxin. The effect of different exchange cations was also minimized in this sample, the reason for which was still not understood yet. The importance of charge density of smectites on aflatoxin adsorption will be further evaluated in layer charge reduction experiments (Chapter 4).

3.3.3 Characterization of Aflatoxin-Smectite Complexes

When synthesizing aflatoxin-smectite complexes on six Ba-saturated clays, the main adsorption for aflatoxin was observed during the first treatment. Total amounts of aflatoxin adsorbed on Ba-saturated clays were 0.73 mol/kg for 1MS, 0.43 mol/kg for 5OK, 0.49 mol/kg for 7AZ, 0.65 mol/kg for 8TX, 0.25 mol/kg for 16MX, and 0.68 mol/kg for 37GR, respectively. Relative abundances of aflatoxin on these clays were in good agreement with adsorption capacities basing on isotherms as reported in 3.3.2.

According to the infrared spectra shown in Figure 3.5, adsorbed aflatoxin B₁ in six complexes showed same band positions and shapes under the same humidity, and their responses to the change of humidity were quite similar. There were differences in band intensities of these complexes, which were proportional to aflatoxin loadings on smectites. Similar infrared spectra suggested that layer charge density of smectites had little or no effect on bonding mechanisms for aflatoxin.

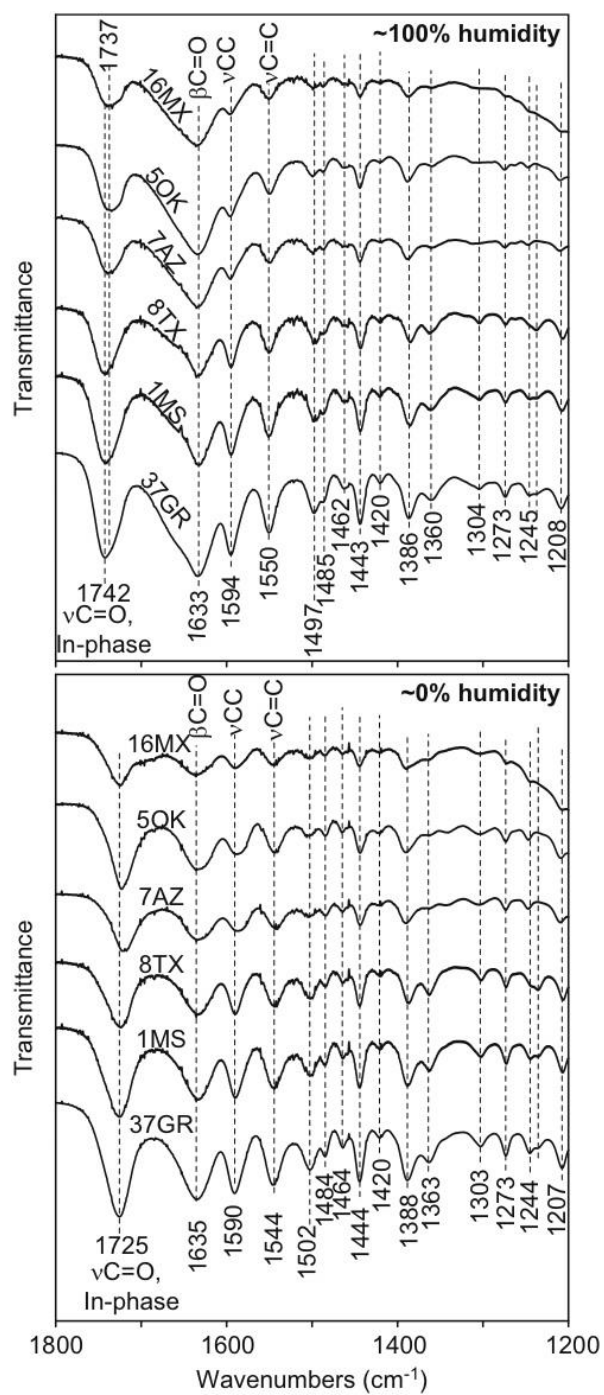


Figure 3. 5: Infrared spectra of aflatoxin-smectite complexes on six clays saturated with Ba, recorded at 0% and 100% humidities, respectively.

Smectites tend to lose interlayer water and collapse at elevated temperatures. As a representative specimen of smectites, sample 37GR collapsed to 1.0 nm in d-spacing when heated to above 150 °C, as shown in Figure 3.6. On the other hand, aflatoxin-smectite complexes could still maintain their d(001)-spacings between 1.25 nm and 1.45 nm even at 300 °C. These higher d-spacings at elevated temperatures suggested that aflatoxin molecules entered interlayers of all six smectites and prevented the mineral from collapsing.

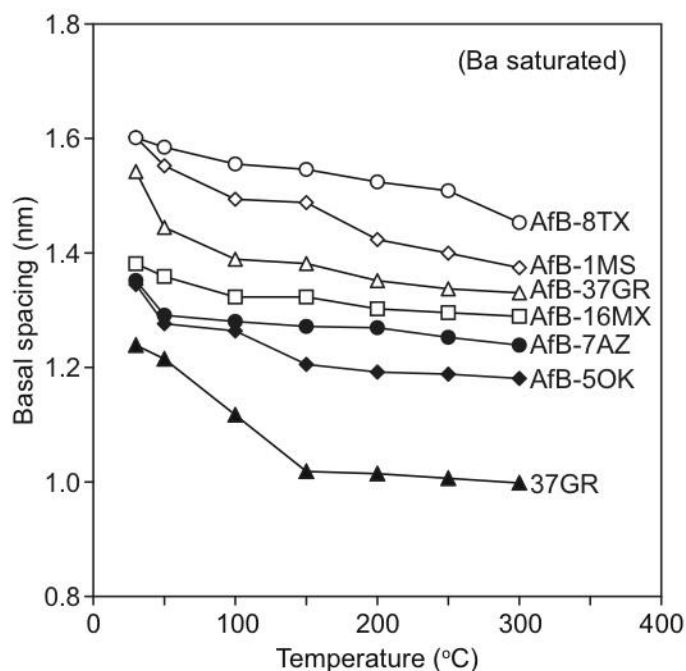


Figure 3. 6: Basal spacings of 37GR clay and six aflatoxin-smectite complexes saturated with Ba, at elevated temperatures.

The XRD analysis also indicated that d-spacings of complexes were roughly proportional to aflatoxin loadings on smectites. It was likely that only some layers of smectites were occupied by aflatoxins, and their random interstratification with AfB₁-

free layers resulted in varied d-spacings. Samples with high aflatoxin loadings were 8TX and 1MS, for which d-spacings reached as high as 1.6 nm at room temperature and maintained greater than 1.4 nm at 300 °C. D-spacings for complexes of 5OK and 7AZ were less than 1.4 nm at room temperature, and collapsed to less than 1.3 nm at 300 °C. The d-spacing of aflatoxin-smectite complex of 16MX was less sensitive to changes in temperatures, which may due to the dilution effect of impurities in this sample.

3.4 Conclusions

Divalent cation saturations of smectites in general resulted in much greater adsorption capacities and affinities for aflatoxin. Cations with smaller hydration radii tended to further enhance the adsorption for aflatoxin. For all six clays, Ba saturation enhanced the size and polarity matching among clay particles, aflatoxin molecules and cations, therefore increased the adsorption when compared with Ca saturation.

All clay samples tested in this study were capable of adsorbing aflatoxin into interlayers. Charge density seemed to have no effect on bonding mechanisms. However, a correlation was observed between cation exchange capacity of smectites and aflatoxin adsorption capacity as well as affinity. The importance of size and polarity matching in the adsorption process will be further verified in charge reduction experiments (Chapter 4).

4. AFLATOXIN ADSORPTION ON CHARGE REDUCED SMECTITES FROM A NATURAL BENTONITE

4.1 Introduction

The correlation between cation exchange capacity of different smectites and their adsorption capacity and affinity for aflatoxin implied the importance of charge density of smectites in aflatoxin adsorption (Chapter 3). The result also suggested that the CEC of smectite as a good adsorbent should be around and less than 110 cmol/kg. The low limit or the optimal CEC value of smectites as good binders, however, could not be determined according to six clay samples tested in Chapter 3, as the low CEC value of 16MX was mainly due to the dilution effect of impurities. More information is needed to correct the above value as selection criteria for smectites as aflatoxin binders.

Cation exchange capacity of most natural smectites falls between 80 and 120 cmol/kg. It is difficult to find smectites with CEC below or at the low end of this range. For the study of aflatoxin adsorption on low CEC smectites, reducing the charge density of natural smectites with chemical methods came out to be a good alternative approach.

The objectives of this part of study were to reduce the CEC of a natural smectite based on the Hofmann and Klemen effects, to test the efficacy of resulting smectites in aflatoxin adsorption, and to determine the optimal charge density of smectites as good binders.

4.2 Materials and Methods

Clay of sample 5OK was chosen for charge reduction tests. The cation exchange capacity of the original 5OK clay was as high as 136.6 cmol(+)/kg, and this clay had the lowest adsorption capacity (Q_{\max}) for aflatoxin among six samples tested. The small affinity constant (K) also indicated that the adsorption of aflatoxin on this clay was very limited at low aflatoxin concentrations.

The predominant mineral in sample 5OK was montmorillonite, a dioctahedral mineral in the smectite group. Described as Hofmann & Klemen effects, cationic Li in interlayers of smectites were able to migrate into vacant octahedral sites after heating, and became part of the layer structure (Jaynes and Bigham, 1987; Jaynes and Boyd, 1991). Octahedral charge imbalance could be partially neutralized in this process, resulting in a smaller cation exchange capacity value of the sample. By quantifying Li in layer structures of charge reduced 5OK clays, it was possible to calculate remaining CEC values of these resulting samples.

4.2.1 Charge Reduction

The clay fraction of sample 5OK was originally saturated by Na during size fractionation. To achieve different charge reduction on the clay, aliquots of this suspension, containing 50 mg of clay each, were treated with mixed solutions of LiCl and NaCl that had 11 varied Na:Li ratios. Exchange cations in interlayers of smectites were partially replaced by Li during the saturation (same procedure as described in 2.1.2), resulting in 11 samples with different Li loadings on exchange sites.

Above clays were transferred into several 50-mL glass beakers, with extra electrolytes removed, and oven dried at 90 °C . Settled dry aggregates were then heated at 250 °C overnight, allowing Li cations to migrate into layer structures of smectites (Jaynes and Bigham, 1987). Care was taken to cool samples gradually and to avoid beaker cracking. After heating, all clay particles aggregated firmly together, and re-dispersion was required for further analysis. Ethanol and water were mixed at 1:1 volume ratio as a dispersion agent of these aggregates. Each of the 250 °C heated sample was immersed into about 25 mL of this mixture. An ultrasonic cleaner was used to assist breaking and dispersing clay aggregates.

Thoroughly dispersed 5OK clays with reduced layer charges were transferred into 50-mL centrifuge tubes, saturated with Ba, and washed with water following procedures described in 2.1.2. Clay content of Ba-saturated clay suspensions was calculated based on weights of clays and water. An adequate amount of each charge reduced clay was transferred into a 15-mL centrifuge tube and diluted to 5 mL to achieve a clay content of 2 mg/mL for adsorption experiment. Aflatoxin adsorption isotherms were measured as described in 3.2.2.

4.2.2 Quantification of Structural Li to Calculate Remaining CEC

After saturation with Ba, it was assumed that charge reduced 5OK clays contained no or little exchangeable Li. By digesting these clay samples with hydrofluoric acid and aqua regia, layer structures were broken down and non-exchangeable Li migrated into vacant octahedral sites would be released into solutions. The Ba-saturated

original 5OK clay without charge reduction was also digested for Li baseline comparison.

Clay digestion was performed in 50-mL centrifuge tubes made of polypropylene, two for each sample. All these tubes were labeled and weighed before use as calculations would be based on weights. Suspensions containing approximately 10 mg of clays were weighed in duplicate, transferred into centrifuge tubes. Concentrated acids (0.15 mL of 69% HNO_3 , 0.45 mL of 39% HCl , and 0.9 mL of 48% HF) were pipetted directly into each tube without dilution. Then tubes were capped and shaken gently for 24 h to make sure that all clays were digested.

When digestion was complete, 15 mL of saturated boric acid was added into each tube to neutralize remaining active HF . These tubes were shaken for another 24 h to dissolve precipitated fluoride compounds of Al, Ca, and other cations. Then 15 mL of 0.05 M NaCl solution was added into the mixture, in order to avoid Li ionization during the atomic emission analysis. Before analysis for Li in these solutions, the weights of tubes with mixtures were recorded. Standard Li solutions were also prepared with digestion reagents and diluted NaCl solution at the same ratio.

4.3 Results and Discussion

Adsorption isotherms for a series of Ba-saturated 5OK clays, including 11 charge reduced samples and the original clay fraction, were fitted well with the exponential Langmuir equation. Reducing layer charges of this smectite clay had a profound impact on AfB_1 adsorption in terms of adsorption affinity, capacity, and isotherm shape as

shown in Figure 4.1. Six adsorption curves were chosen as representatives and plotted together, with CEC values of clays marked in this figure.

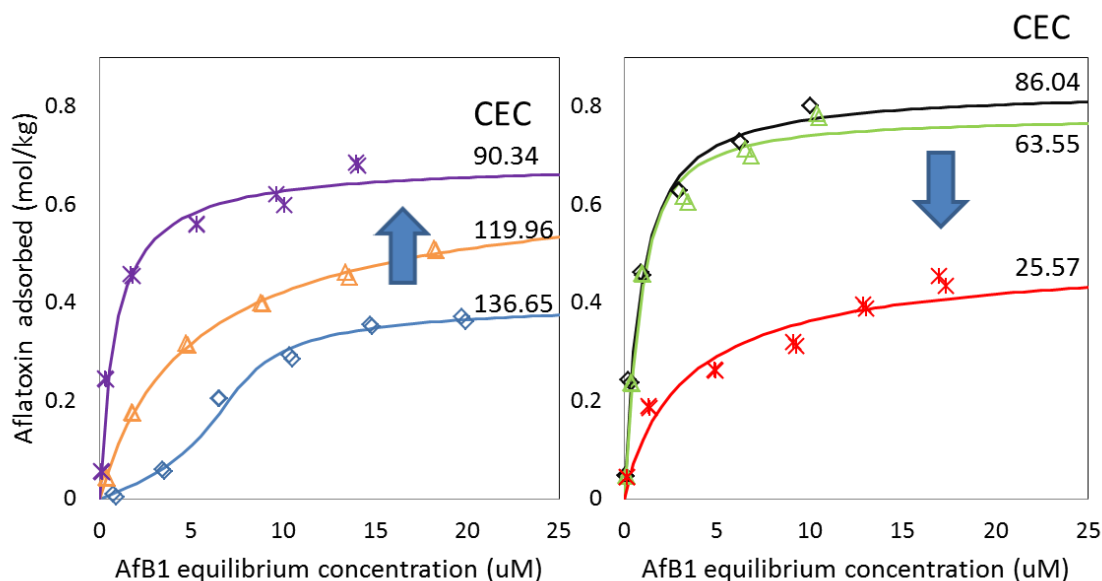


Figure 4. 1: AFB1 adsorption on charge reduced 5OK clays saturated with Ba. (CEC unit: cmol(+)/kg)

Original clay fraction of 5OK showed low adsorption capacity and affinity for aflatoxin in previous tests, and its CEC reached up to 136.6 cmol(+)/kg. With layer charges partially reduced, aflatoxin adsorption was enhanced significantly, indicated by elevated platforms and steep slopes of adsorption isotherms. When CEC values were between 63 and 90, the isotherm curves showed typical L-shapes, indicating high affinity of the smectites for aflatoxin. However when the charge density was reduced by more than a half of the original value, both of the adsorption capacity and affinity decreased again. Curve fittings for isotherms of all modified clays were also improved,

with altered shapes as indicated above. Aflatoxin adsorption capacities and affinity constants of 12 clay samples from 5OK were shown in Figure 4.2.

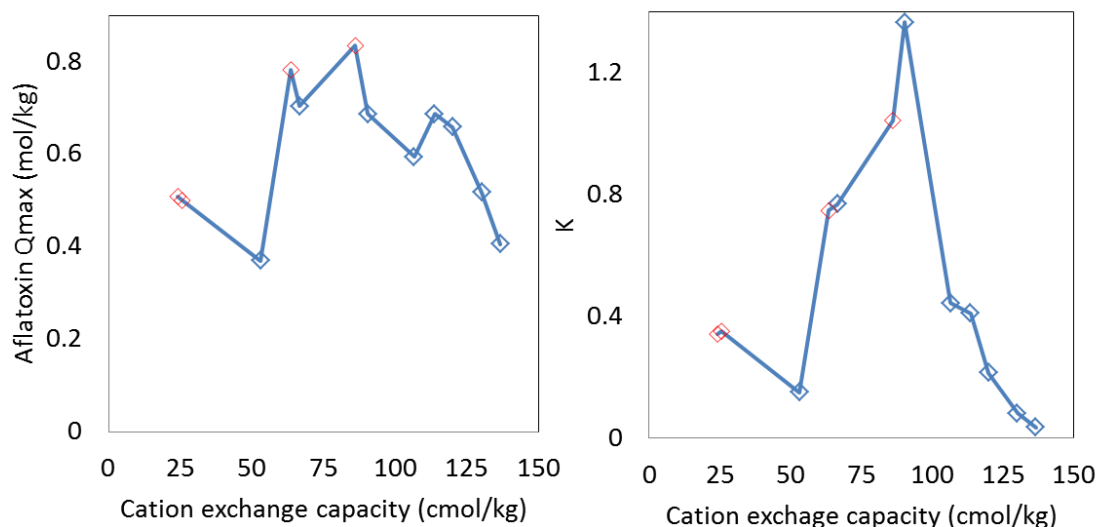


Figure 4. 2: AfB1 adsorption capacity & affinity on charge reduced 5OK clays.

Blue points in Figure 4.2 represented samples tested in the first trial, and red points were from the second trial. Samples with lower charge density tend not to disperse well after heating, which may affect aflatoxin adsorption. This problem was solved in the second trial with the help of an ultrasonic cleaner. It can be concluded from this figure, that a CEC between 80 and 110 cmol(+)/kg made smectite a good binder for aflatoxin.

This study verified that cation exchange capacity was a crucial factor to consider when selecting smectite clays for aflatoxin adsorption. High tendency of forming pseudo-crystals in high-charge density smectites would hinder their accessibility of the

interlayer space (McBride, 1994) and induce high energy barriers to initiate interlayer aflatoxin adsorption. In addition, crowded exchange cations with associated water in interlayers of smectites with high CEC would prohibit aflatoxin molecules to occupy hydrophobic surfaces on the clay. On the other hand, the bonding between cations and aflatoxins was reduced in samples with low charge density, since the quantity of exchange cations was much less than in the natural clay. Another problem for low CEC samples was that 2:1 layers tend to stick together and they hardly get dispersed in water, therefore, the accessibility for aflatoxins was limited. These results further supported previous conclusions in 3.3.2.

4.4 Conclusions

Charge reduction of a natural smectite with relatively high CEC through the Hofmann and Kelment effects could alter its ability for aflatoxin adsorption. An increasing and then decreasing trend in both adsorption capacity and affinity was observed when the CEC of clay 5OK was reduced from 136.7 cmol(+)/kg to 25.6 cmol(+)/kg. The effectiveness of modified samples reinforced the importance of charge density in determining the adsorption process. For aflatoxin detoxification, the optimal CEC of a smectite should fall in the range between 80 and 110 cmol(+)/kg. Within this range of charge density, both of the clay's adsorption capacity and affinity for aflatoxin could be maximized.

5. SUMMARY

Six bentonites analyzed in this study were all classified as clay in texture. Smectite was identified as the dominant mineral in clay fractions of all six samples, while sample 16MX also contained some impurities of kaolinite and albite. According to differences in CEC values of clays, these six samples could be classified into three groups: two samples with high CEC (5OK, 7AZ), three with moderate CEC (1MS, 8TX, 37GR) and one sample with low CEC (16MX).

Divalent cation saturations of smectites in general resulted in much greater adsorption capacities and affinities for aflatoxin. Cations with smaller hydration radii tended to further enhance the adsorption process for aflatoxin on smectites. For all six clays, Ba saturation enhanced the size and polarity matching among clay particles, aflatoxin molecules and cations, therefore increased the adsorption when compared with Ca saturation.

All clay samples tested in this study were capable of adsorbing aflatoxin into interlayers, and the charge density seemed to have no effect on bonding mechanisms. However, a correlation was observed between cation exchange capacity of smectites and their aflatoxin adsorption capacity as well as affinity.

Charge reduction for a natural bentonite with relatively high CEC could alter its behavior in aflatoxin adsorption. The effectiveness of modified samples reinforced the important role of charge density in determining the adsorption process. For the purpose of aflatoxin detoxification, a smectite with cation exchange capacity between 80 and 110

cmol(+)/kg could be a good candidate. Adequate charge density could maximize aflatoxin adsorption on smectites, with both capacity and affinity enhanced.

REFERENCES

- Abdel-Wahhab, M. A., Nada, S. A., and Amra, H. A. (1999). Effect of aluminosilicates and bentonite on aflatoxin-induced developmental toxicity in rat. *Journal of Applied Toxicology*, **19**, 199-204.
- Arriola, M. C., Porres, E., Cabrera, S., Zepeda, M., and Rolz, C. (1988). Aflatoxin fate during alkaline cooking of corn for tortilla preparation. *Journal of Agricultural and Food Chemistry*, **36**, 530-533.
- Bailey, C. A., Latimer, G. W., Barr, A. C., Wigle, W. L., Haq, A. U., Balthrop, J. E., and Kubena, L. F. (2006). Efficacy of montmorillonite clay (Novasil plus) for protecting full-term broilers from aflatoxicosis. *The Journal of Applied Poultry Research*, **15**, 198-206.
- Brekke, O. L., Sinnhuber, R. O., Peplinski, A. J., Wales, J. H., Putnam, G. B., Lee, D. J., and Ciegler, A. (1977). Aflatoxin in corn: Ammonia inactivation and bioassay with rainbow trout. *Applied and Environmental Microbiology*, **34**, 34-37.
- Deng, Y., Barrientos Velazquez, A. L., Billes, F., and Dixon, J. B. (2010). Bonding mechanisms between aflatoxin B₁ and smectite. *Applied Clay Science*, **50**, 92-98.
- Deng, Y. and Szczerba, M. (2011). Computational evaluation of bonding between aflatoxin B₁ and smectite. *Applied Clay Science*, **54**, 26-33.
- Deng, Y., White, G. N., and Dixon, J. B. (2009). Soil mineralogy laboratory manual. Texas A&M University, College Station.

- Eisenhour, D. D. and Brown, R. K. (2009). Bentonites and its impact on modern life. *Elements*, **5**, 83-88.
- Ellis, R. W., Clements, M., Tibbetts, A., and Winfree, R. (2000). Reduction of the bioavailability of 20 µg/kg aflatoxin in trout feed containing clay. *Aquaculture*, **183**, 179-188.
- Grant, P. G. and Phillips, T. D. (1998). Isothermal adsorption of aflatoxin B1 on HSCAS clay. *Journal of Agricultural and Food Chemistry*, **46**, 599-605.
- Grove, M. D., Plattner, R. D., and Weisleder, D. (1981). Ammoniation products of an aflatoxin model coumarin. *Journal of Agricultural and Food Chemistry*, **29**, 1161-1164.
- Guevara-Gonzalez, R. G. (2011). Aflatoxins – biochemistry and molecular biology. Texas Tech University, Lubbock.
- Herrera, M., Zyman, J., Pena, J. G., Segurajauregui, J. S., and Vernon, J. (1986). Kinetic studies on the alkaline treatment of corn (*Zea mays*) for tortilla preparation. *Journal of Food Science*, **51**, 1486-1490.
- Jaynes, W. F. and Bigham, J. M. (1987). Charge reduction, octahedral charge, and lithium retention in heated, Li-saturated smectites. *Clays and Clay Minerals*, **35**, 440-448.
- Jaynes, W. F. and Boyd, S. A. (1991). Hydrophobicity of siloxane surfaces in smectites as revealed by aromatic hydrocarbon adsorption from water. *Clays and Clay Minerals*, **39**, 428-436.

- Kannewischer, I., Tenorio, A. M. G., White, G. N., and Dixon, J. B. (2006). Smectite clays as adsorbents of aflatoxin B₁: Initial steps. *Clay Science*, **12**(Supplement 2), 199-204.
- Lindemann, M. D., Blodgett, D. J., Kornegay, E. T., and Schurig, G. G. (1993). Potential ameliorators of aflatoxicosis in weanling growing swine. *Journal of Animal Science*, **71**, 171-178.
- McBride, M. B. (1994). Environmental chemistry of soils. Oxford University Press, New York.
- Mulder, I., Tenorio, A. M. G., White, G. N., and Dixon, J. B. (2008). Smectite clay sequestration of aflatoxin B₁: Mineral dispersivity and morphology. *Clays and Clay Minerals*, **56**, 559-571.
- Murphy, P. A., Hendrich, S., Landgren, C., and Bryant, C. M. (2006). Food mycotoxins: An update. *Journal of Food Science*, **71**, 51-65.
- Odom, I. E. (1984). Smectite clay minerals: Properties and uses. *Philosophical Transactions of the Royal Society of London A*, **311**, 391-409.
- Phillips, T. D., Kubena, L. F., Harvey, R. B., Taylor, D. R., and Heidelbaugh, N. D. (1988). Hydrated sodium aluminosilicate: A high affinity sorbent for aflatoxin. *Poultry Science*, **67**, 243-247.
- Phillips, T. D., Sarr, A. B., and Grant, P. G. (1995). Selective chemisorption and detoxification of aflatoxins by phyllosilicate clay. *Natural Toxins*, **3**, 204-213.
- Pimpukdee, K., Kubena, L. F., Bailey, C. A., Huebner, H. J., Afriyie-Gyawu, E., and Phillips, T. D. (2004). Aflatoxin-induced toxicity and depletion of hepatic

- vitamin A in young broiler chicks: Protection of chicks in the presence of low levels of Novasil Plus in the diet. *Poultry Science*, **83**, 737-744.
- Scheideler, S. E. (1993). Effects of various types of aluminosilicates and aflatoxin B₁ on aflatoxin toxicity, chick performance, and mineral status. *Poultry Science*, **72**, 282-288.
- Schell, T. C., Lindemann, M. D., Kornegay, E. T., Blodgett, D. J., and Doerr, J. A. (1993). Effectiveness of different types of clay for reducing the detrimental effects of aflatoxin-contaminated diets on performance and serum profiles of weanling pigs. *Journal of Animal Science*, **71**, 1226-1231.
- Squire, R. A. (1981). Ranking animal carcinogens: A proposed regulatory approach. *Science*, **194**, 877-880.
- Tenorio, A. M. G., Mulder, I., and Dixon, J. B. (2008). Smectite clay adsorption of aflatoxin vs. octahedral composition as indicated by FTIR. *Clays and Clay Minerals*, **56**, 571-578.
- Viani, A., Gualtieri, A. F., and Artioli, G. (2002). The nature of disorder in montmorillonite by simulation of X-ray powder patterns. *American Mineralogist*, **87**, 966-975.
- Zain, M. E. (2011). Impact of mycotoxins on humans and animals. *Journal of Saudi Chemical Society*, **15**, 129-144.